33RD CONGRESS
OF THE INTERNATIONAL COUNCIL
OF THE AERONAUTICAL SCIENCES
STOCKHOLM, SWEDEN, 4-9 SEPTEMBER, 2022

ICAS 2022 SWEDEN

VALIDATING AIRSPACE CFD MODELS FOR DRONE OPERATION WITH FLIGHT TEST DATA

David Standingford[1], Carl Sequeira[2], Mark Allan[1], Conrad Rider[2], Gabriel Furse[2] & James Sharpe[1]

[1]Zenotech Ltd, 1 Larkfield Grove, Chepstow, Monmouthshire NP16 5UF, UK
[2]Flare Bright Ltd, The Stable Yard, Vicarage Road, Milton Keynes, Buckinghamshire MK11 1BN, UK

Abstract

Wind modelling of urban and airport sites is a crucial element in the new landscape of UAV operation and data systems. Accurate, highly localised wind models are critical to adoption, as are the wind measurement tools necessary to validate such models. We present here a comparison between RANS and IDDES CFD model results, static anemometer data and live flight trials of the SnapShot wind measurement nano-glider close to large buildings at Cardiff International Airport. The results indicate very good correlation between the CFD results and the experimental flight test data, demonstrating a route to accurate validation of localised flow models to aid future UAV operation.

Keywords: drone, wind, urban airspace, aerodynamics, CFD

1. Motivation - the need for validated airspace modelling

The global market for drones, advanced air mobility (AAM) and supporting services is circa $74billion by 2035 [9] with the forecast market for services £4billion. UKRI [10] concludes that the case for change from the baseline services is sound in inspection, delivery, and sub-regional air-taxis. All operators need safety and have commercial requirements for insurance to fly. Specific sites require specialist aerodynamic effects modelling. Meso-scale data suppliers include the UK Met Office that offers a UK Atmospheric Hi-Res Model with spatial resolution of approximately 2km with wind speed and direction at 10.0m height above ground level. This is well suited to the planning and execution of drone and other aircraft flights in open terrain, but it does not include the localised aerodynamic features (vortices and shear layers) that are required for the safe operation of aircraft in the urban environment. While more localised models can be produced, as with any simulation-based dataset, the method and model must be validated using independent data sources. For complex, highly structured flows, as expected in urban environment validation data is hard to come by using traditional static anemometers. In this paper, we present the validation of high-resolution CFD models using flight test data from a novel wind measurement nano-drone system to produce accurate, localised aerodynamic data sets for specific operational sites.

2. The production of localised aerodynamic datasets

The aerodynamic dataset is based on a 25km^2 area computational fluid dynamics (CFD) model based on a combination of building geometry from AccuCities and the LiDAR Composite Dataset available from Natural Resource Wales [13], shown in Figure 1. The CFD dataset is produced for a range of wind speeds and directions from meso-scale sources with steady and unsteady models to account for primary wind speed and gusts. We use a fully turbulent air model within the parallel GPU-enabled zCFD solver [1], [2], [3] and unstructured overset meshes to streamline future buildings and geometry updates.

2.1 CFD model

The computational fluid dynamics (CFD) simulation is based on a 5km x 5km domain to a height of 10km. The terrain data is obtained from the DEFRA LIDAR digital terrain map (DTM) survey, with 2.0m spacing [13]. Added to this are building geometries commercially obtained from AccuCities, including all main buildings on the Cardiff International Airport site and surrounds, as shown in Figure 1. Additional buildings are obtained from the OpenStreetMap database. All sources are mapped to the EPSG:27700 projection for consistency.

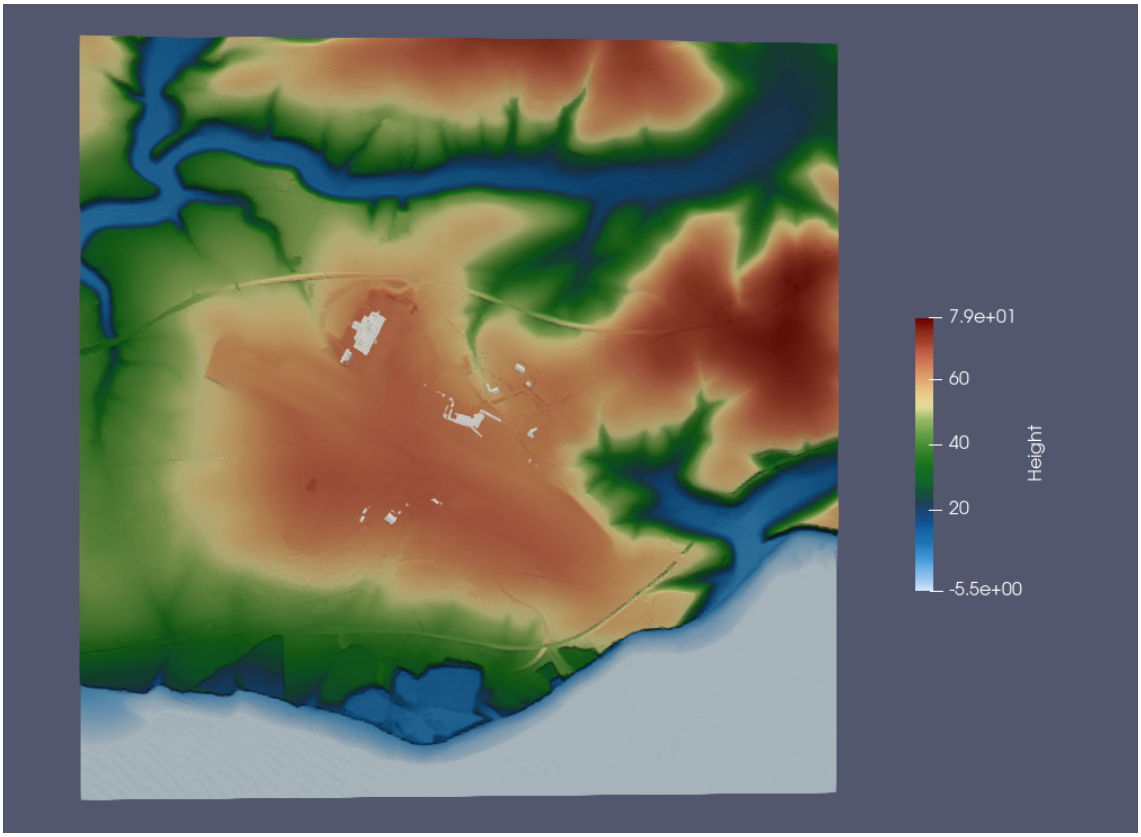

Figure 1 – Overview of the Cardiff International Airport location in South Wales, showing the elevation in metres above mean sea level (MSL) as per the Natural Resource Wales LIDAR Composite Dataset. The key buildings are shown in white, including the terminal building, the British Airways maintenance hangar and various nearby service buildings.

The terrain mesh covering the entire flow domain is designed to capture the atmospheric boundary layer (ABL) and is automatically spaced between 10.0m and 25.0m horizontally on the ground according to the slope, height, and curvature of the terrain. The vertical mesh spacing is 1.0m at ground level with a vertical expansion ratio of 1.2 up to the maximum spacing of 100.0m. The resulting terrain mesh has circa 10m cells. The 107 bounding boxes for the individual buildings shown in Figure 2 are aggregated prior to meshing into 7 super-blocks. Each super-block is meshed with an octree using the CAAMesh functionality in zCFD, refined to 1.0m near buildings. With the overset blocks, the complete mesh has 60m cells

To produce roughness type information, we image-process satellite data to create the colour map shown in Figure 3.

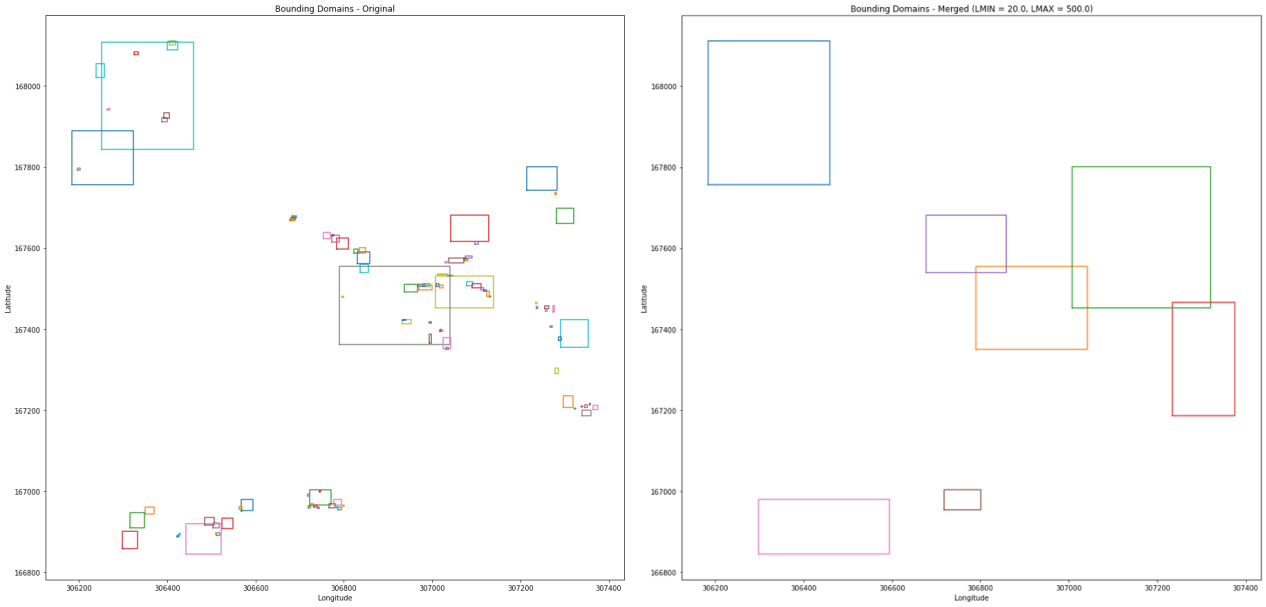

Figure 2 – (Left) the original 107 bounding boxes for the individual buildings. (Right) 7 aggregated super-blocks. The large blue block at the top left of the right figure is the British Airways (BA) Maintenance Hangar (and surrounds).

Figure 3 – Colour classification of terrain type (blue = water, light brown = built up area, dark green = trees, dark grey = road / tarmac, light green = grass and similar). The colours are automatically converted into a roughness length map for the terrain as per Table 1.

This data is used directly by the zCFD solver as a wall function boundary condition on the ground. The boundary conditions for each wind speed and direction considered are generated as vertical profiles offset to the local ground height, corresponding to homogeneous turbulence atmospheric boundary layers (ABL) matching the meso-scale wind speed at a height above ground of 10.0m. The farfield boundary conditions are applied

by the solver with Riemann conditions that automatically switch to the ABL condition when the flow is into the domain, with extrapolation when the flow is out of the domain. The ground boundary condition is a turbulent wall-function with roughness length based on the terrain type, as per Table 1. The solver has a density-based explicit finite volume / high order Discontinuous Galerkin formulation with low Mach number preconditioning. CFD model parameters are set according to Table 2.

Terrain type	Roughness length (m)
Water	0.0002
Trees	0.5
Road	0.0024
Built-up	1.0
Grassland	0.05

Table 1 – Length scales for terrain types used in the CFD model, following Landberg [14].

Parameter	Value
Pressure	101325 Pa
Temperature	273.15 K
Eddy viscosity ratio	0.1
Turbulence intensity	0.01
Viscosity	1.79e-5 Pa.s
Prandtl No	0.72
Sutherland's constant	110.4
Turbulent Prandtl No	0.9
Ratio of specific heats (gamma)	1.4
Gas constant	287.0
CFL number (explicit)	1.0
Cycles	3000
Multigrid	Level 2
Scheme	Runge-Kutta Level 5
Turbulence	Menter SST (beta* =0.03)

Table 2 – Parameter settings for CFD solver.

3. Meso-scale wind data

To index the pre-calculated CFD data we use a meso-scale historical and forecast wind speed and direction data service called Skylink [11].

4. Validation using static anemometers

To provide time-averaged validation data at a specific location, we have generated a RANS dataset covering the entire domain with farfield (ABL) stable wind conditions at 15-degree increments (24 wind directions) each at 3 wind speeds (2.5m/s, 5.0m/s and 7.5m/s). The simulations were run to convergence in so far as the flow field was fully developed and further iteration did not materially change the flow field. An agricultural anemometer from Sencrop was installed at the location indicated in Figure 4. The anemometer is connected to the SIGFOX communications network plus a cloud-based data portal, and has a 3-year battery life, making it ideal for longer-term studies with remote data access.

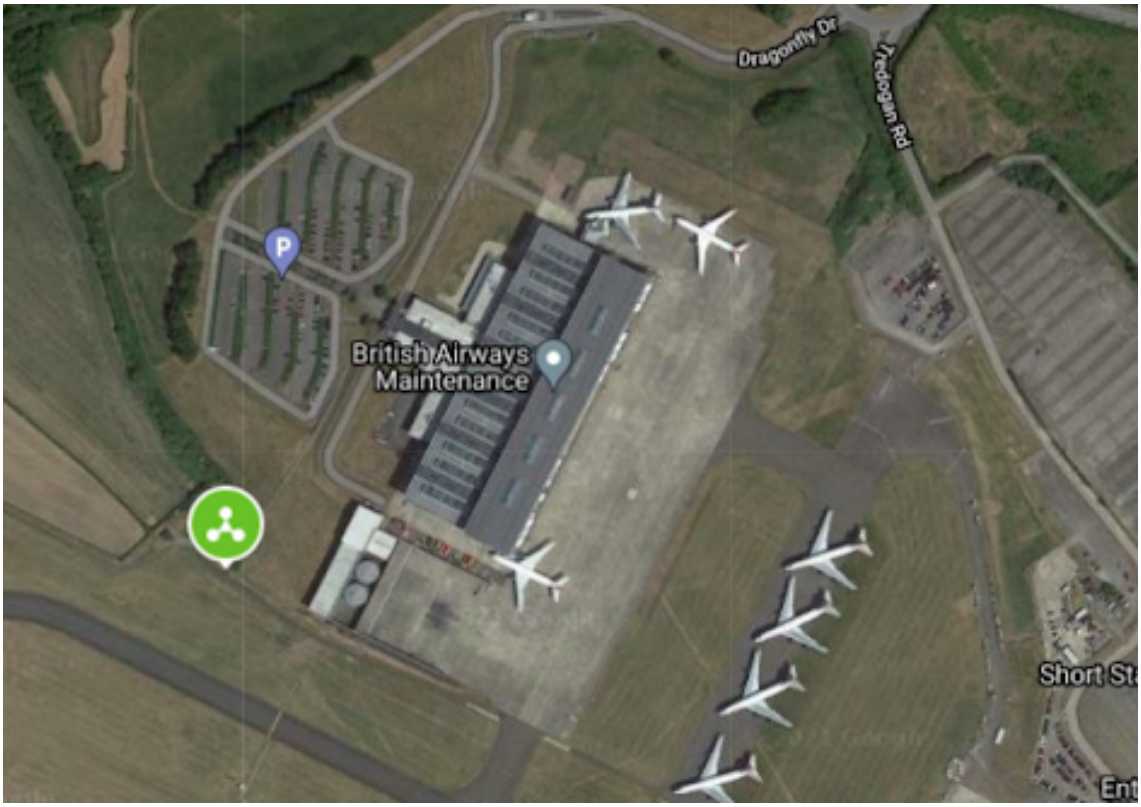

Figure 4 – location (green circle) of the Sencrop anemometer “Zenotech001” close to the BA Maintenance Hangar at Cardiff International Airport. The location has been chosen so that measurements will be significantly impacted by the building, with differing influences depending upon the meso-scale conditions (wind speed and direction).

A comparison of the wind speed measured and predicted for the duration of the flight trial is presented in Figure 5 with the wind direction shown in Figure 6. The measured wind speed is significantly different from the un-disturbed meso-scale data (‘Skylink'). The RMS error between the model and measurements is less than 1.0 m/s over the 35-hour period considered and the RMS error in the wind direction is 5 degrees. Further work is planned to establish the correlation over a longer time-period.

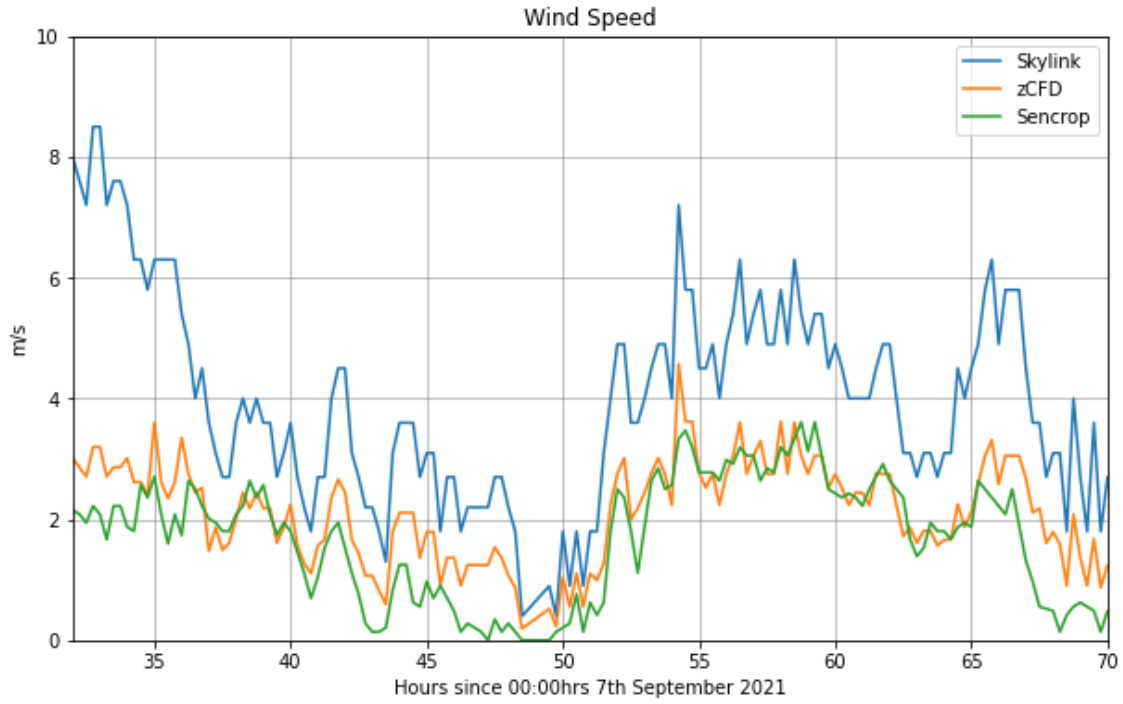

Figure 5 – Comparison between the predicted ("zCFD") and measured ("Sencrop") wind speed at the location of the Sencrop anemometer based on the Skylink meso-scale conditions ("Skylink").

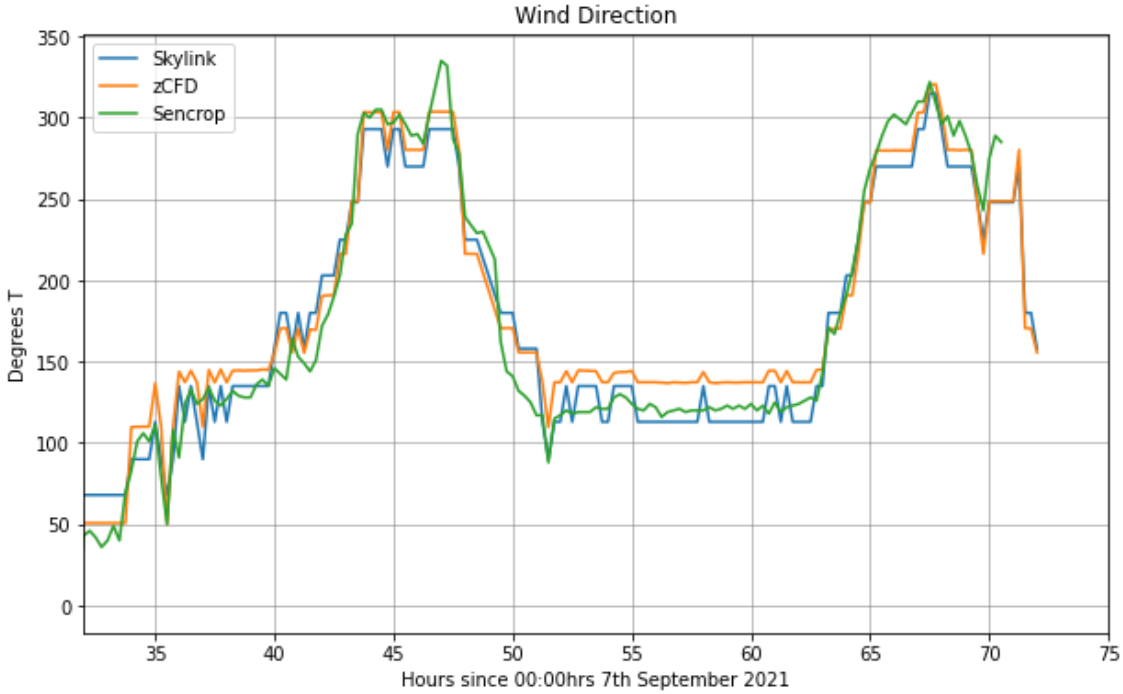

Figure 6: Comparison between the predicted ("zCFD") and measured ("Sencrop") wind direction at the location of the Sencrop anemometer based on Skylink meso-scale conditions ("Skylink").

5. Production of flight test wind measurement data

Flight test wind measurement data has been produced using Flare Bright's bespoke nano-drone, SnapShot (Figure 7). SnapShot is a gliding, unpowered, autonomous drone, weighing 90g and sized to fit within a 100x100x70mm box. SnapShot is a unique flying wind

measurement device, designed to measure 3D real time unsteady wind data at frequencies higher than 200Hz without reliance on typical aircraft-based airspeed tools, such as pitot probes.

The drone is launched vertically from the ground, using a pneumatic launcher, and will measure wind along its ascent path, before autonomously flying back to the user like a boomerang. This allows a vertical profile of the instantaneous unsteady wind condition to be measured – a 'SnapShot' of the wind. The apogee of flight is determined by the pressure of the launch system, as the drone itself is unpowered except for limited supercapacitors necessary to power the control surfaces. With the launch capability at the time of test, SnapShot could fly up to a maximum apogee of approximately 65m, although the aircraft can loop earlier in different winds to achieve the necessary control to return to the user. These flight decisions are made autonomously, such that the only training the operator needs is on the safe operation of a ground based pneumatic launch system not too dissimilar from a tripod mounted flare gun – Figure 8 shows SnapShot being launched.

Consequently, with minimal training requirements and a simple 'press button' launch system, SnapShot provides a means of measuring detailed unsteady wind profiles in complex flow environments where static anemometers would provide insufficient information for safe drone operation or would be too expensive to install.

Figure 8: SnapShot drone used at Cardiff Airport wind measurement trials

Figure 9: SnapShot in flight moments after launch, photographed from under the launcher

Flight test data has been gathered at two launch sites airside at Cardiff Airport near the British Airways Maintenance Hangar in a range of wind conditions, chosen, where possible, to ensure the data gathered was downstream of the building given the prevailing meso-scale wind direction. These sites are indicated in Figure 9 along with the location of the reference Sencrop anemometer. In the following sections, this data is compared extensively with CFD data of increasing levels of fidelity both to validate the CFD models itself but also to illustrate the realism and accuracy of the SnapShot flight test-based wind measurement system. Further work is ongoing to independently verify the accuracy of SnapShot as a wind measurement system.

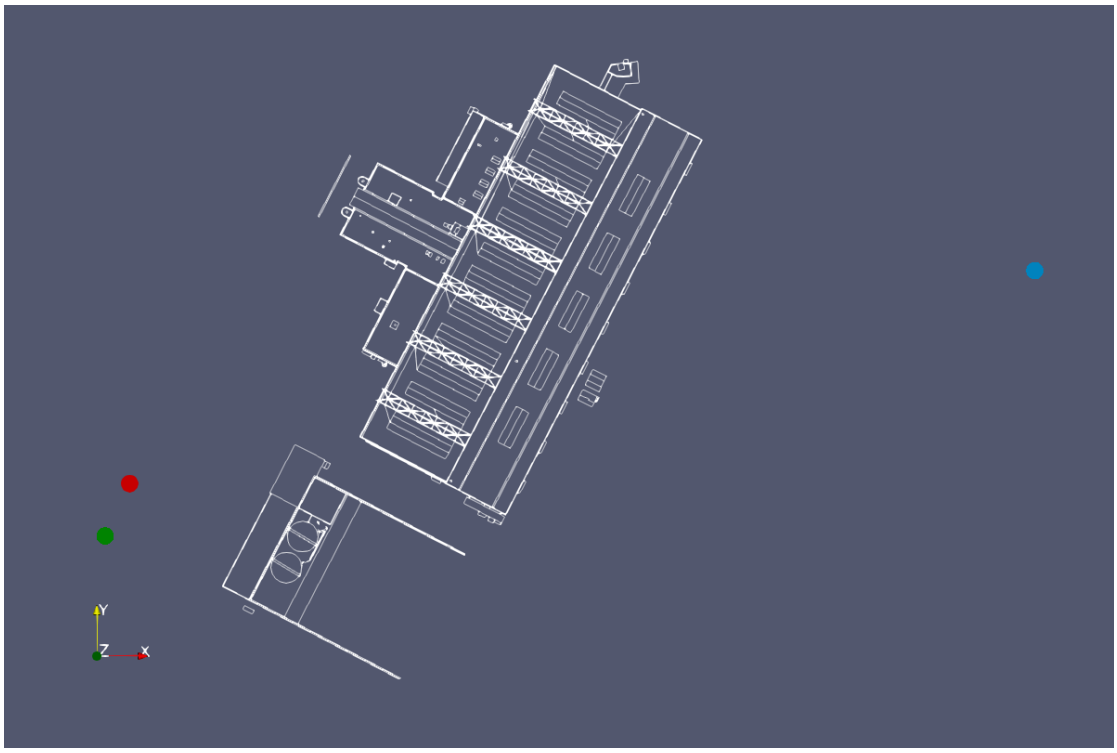

Figure 9: Locations and EPSG:27700 projection co-ordinates of the launch location A (blue, [306550,167990]), launch location B (red, [306131, 167868]) and the Sencrop anemometer (green, [306117, 167838]) in proximity to the BA Maintenance Hangar (white outline).

6. Validation of RANS CFD with flight test data

The Reynolds-averaged Navier Stokes (RANS) dataset can be used as the basis for comparison with the SnapShot drone data by extracting vertical profiles from the CFD domain at the SnapShot launch location. The CFD data for each specific launch is linearly interpolated from the 72-simulation dataset (24 wind directions, 3 wind speeds at each direction) based on the meso-scale conditions. The 4 closest datapoints in (windspeed, wind direction) space are used as the basis for interpolation. The resulting velocity profile is the weighted sum of the profiles extracted from the CFD dataset. We compare the profile data from the SnapShot drone while in ascent.

6.1 Launch location A

The flight tests for the first launcher location were broadly divided into two groups where the wind was dominantly from the west (270T) and the south (180T). The qualitative difference between the two wind directions is that wind from the west passes over the BA Maintenance Hangar before it reaches the launch location, and wind from the south does not (though it is diverted around the building). Flights from the south were characterised by velocity profiles

as illustrated in Figure 10. Flights from the west are characterised by the velocity profiles as illustrated in Figure 11.

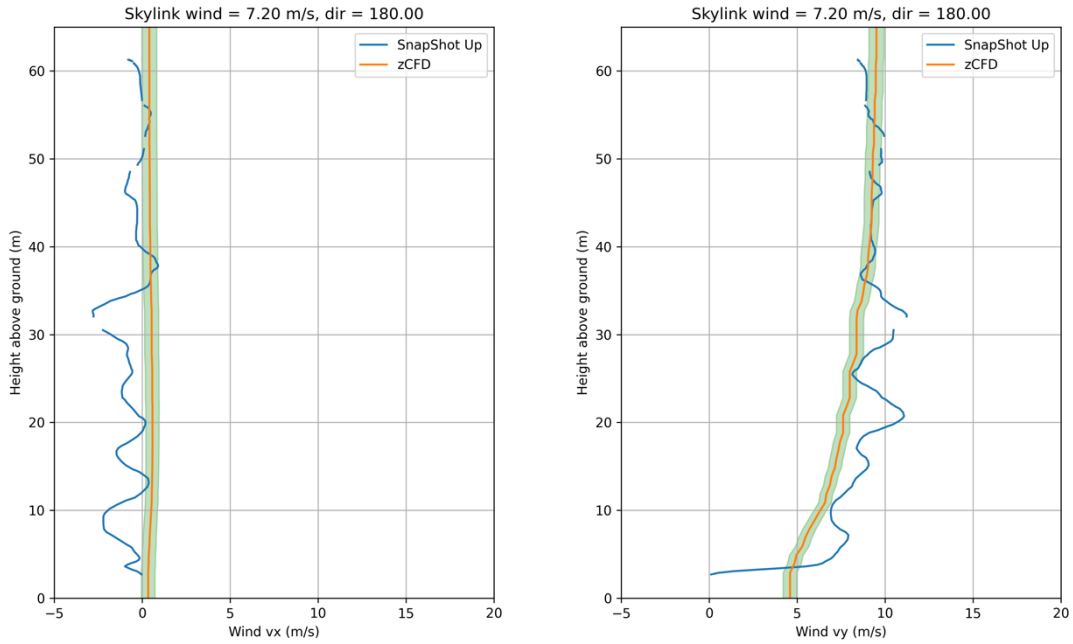

Figure 10: Velocity profile comparison between SnapShot and the RANS CFD dataset for launch location A, with the prevailing wind from the south (180T). The x-component (left) and y-component (right) are in good overall agreement, noting that there is structure in the flow detected by SnapShot that is averaged out in the RANS CFD data.

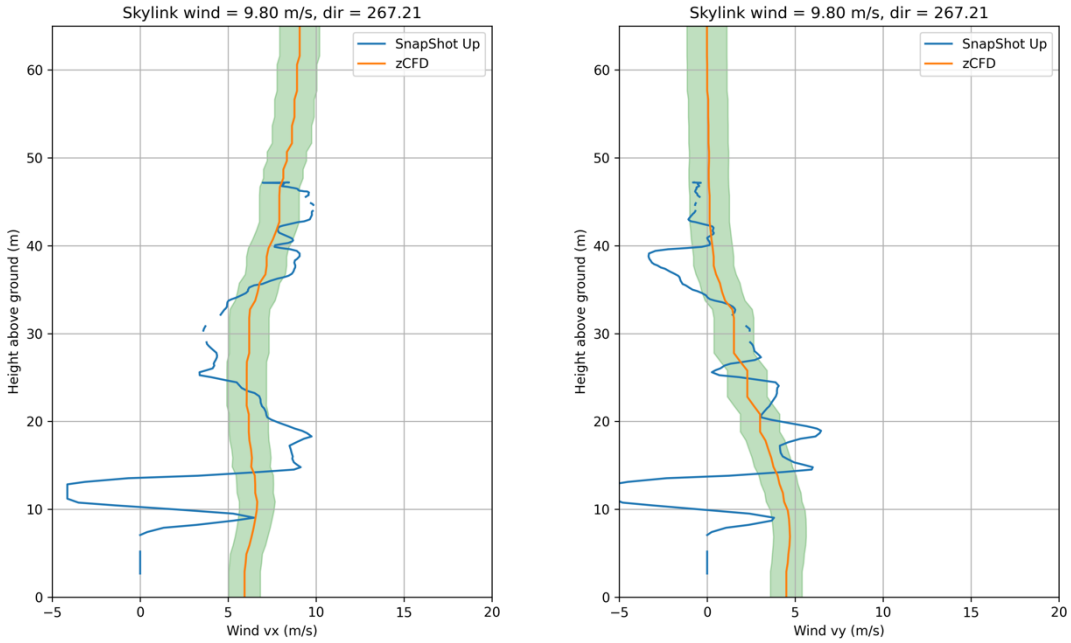

Figure 11: Velocity profile comparison between SnapShot and the RANS CFD dataset for launch location A, with the prevailing wind from the west (270T). The x-component (left) and y-component (right) are in reasonable overall agreement, however the high level of energy in the unsteady flow structure is clear in the SnapShot data. Note that linear

extrapolation to 9.80 m/s for the meso-scale conditions have been based on the pre-calculated RANS CFD data for 7.5 m/s.

In each case the (orange) RANS CFD data line has an error bar in green corresponding to the turbulence kinetic energy modelled by the RANS CFD:

$$\Delta v_i = \frac{1}{3}|v|.I$$

The turbulence intensity *I* is calculated by the RANS solver and the velocity components v_i are in the *x, y,* and *z* directions respectively. The turbulence kinetic energy margins on the RANS CFD solution are notably larger in Figure 11 than Figure 10, as the highly turbulent air has passed directly over the BA Maintenance Hangar.

6.2 Launch location B

Several flights were launched from location B, which is airside in the manoeuvring area to the south-east of the BA Maintenance Hangar. Most of the flights had a prevailing wind from the east (90T) characterised by velocity profiles as illustrated in Figure 12.

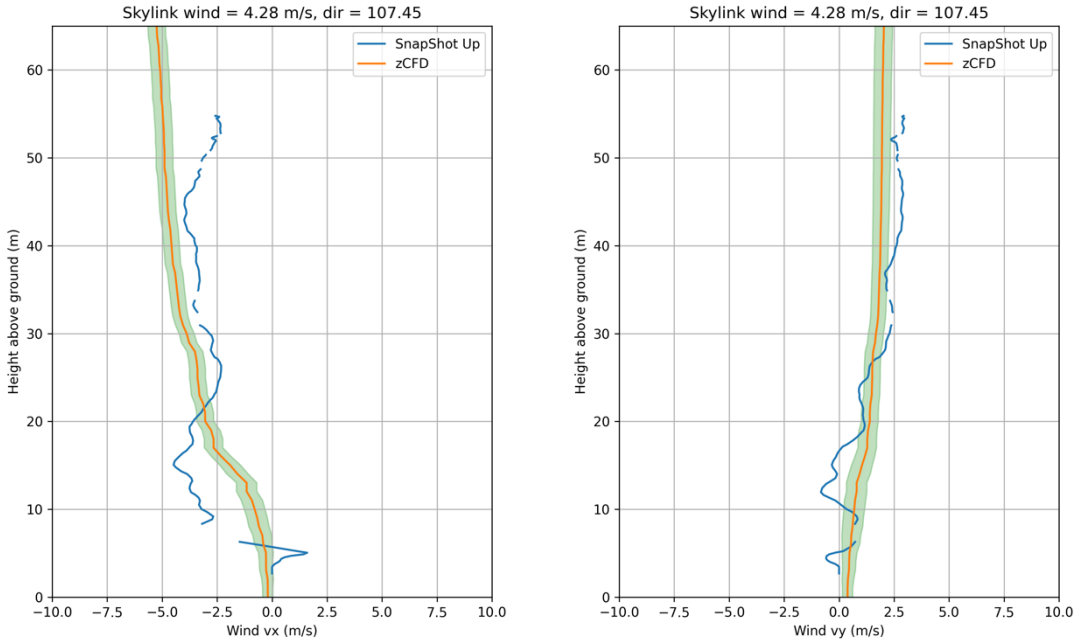

Figure 12: Velocity profile comparison between SnapShot and the RANS CFD dataset for launch location B, with the prevailing wind from the east (90T). The x-component (left) and y-component (right) are in reasonable overall agreement, noting that SnapShot is sensitive to flow features that are averaged out in the RANS CFD data.

7. Validation of (I)DDES CFD with flight test data

The preceding section compared RANS CFD data with SnapShot measured wind data to show that there is good overall agreement, however the unsteady and turbulent flow features detected by SnapShot require a scale resolving CFD simulation to provide a correlation. We use an unsteady Improved Delayed Detached Eddy Simulation (IDDES) model [12] run for a

2-minute physical time-period with a time-step of 0.1s. The parameters used, in addition to the RANS CFD simulations, are listed in Table 3.

Parameter	Value
Real timestep	0.1s
Total time	120.0s
Integration	Dual time-stepping
Inner cycles (local time-stepping)	50
Spatial order	2
Turbulence	IDDES
Cd1	20.0
Cd2	3
Cw	0.15

Table 3 – Parameter settings for CFD solver.

An unsteady flow field corresponding to the IDDES simulation is shown in Figure 11. The complex flow structures downstream of the hangar, identified in the IDDES solution, are clearly not well represented by the RANS CFD velocity profiles shown in Figures 10-12.

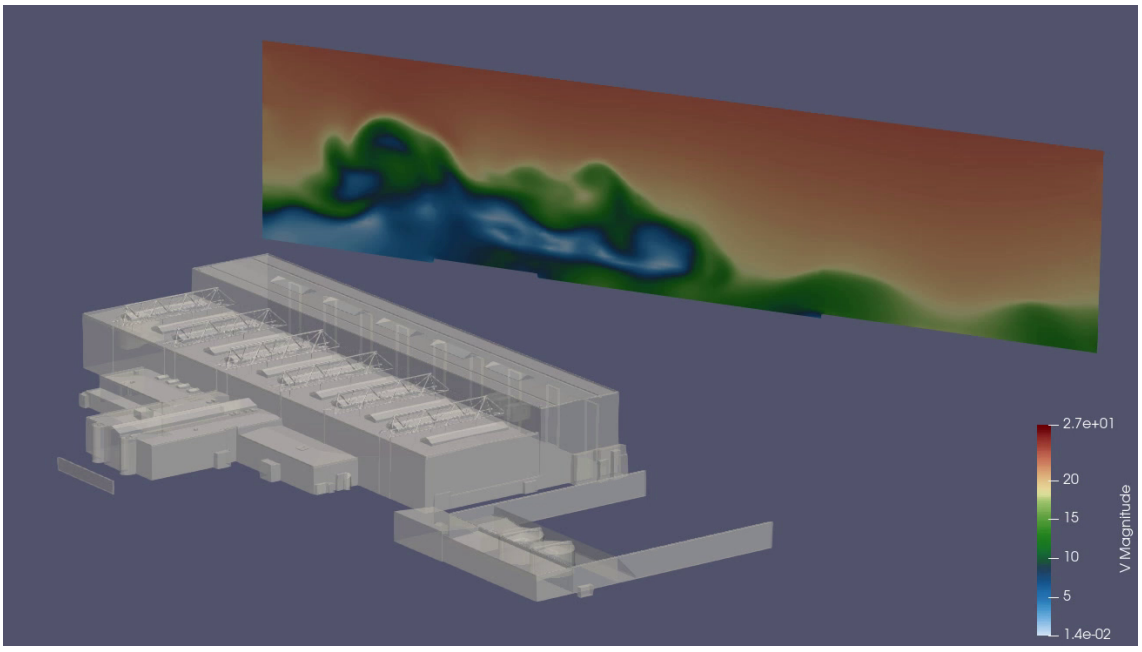

Figure 13: Unsteady velocity magnitude slice through the IDDES CFD flow field with the prevailing wind from the west (270T). The slice is located on the leeward side of the BA Maintenance Hangar and includes launch location A.

To compare the unsteady IDDES CFD data with the SnapShot measured data we introduce the Ensemble Fourier Transform (EFT) for the IDDES velocity profiles at the launch location:

$$MEAN(EFT_i) = \frac{1}{N}\sum_{j=1}^{N} FFT(v_{ij})$$
$$STD(EFT_i) = STD(FFT(v_{ij}))$$

Where *FFT* is the Fast Fourier Transform of the vertical velocity profile sampled at 1.0m spacing and *STD* is the standard deviation of the *FFT* applied to each of the IDDES profiles in a set. The velocity component is indicated as i = 1, 2 and 3 for x, y, and z, where the co-ordinate system is aligned with the EPSG:27700 projection. The authors note that such a decomposition is somewhat arbitrary and that the components are correlated. Investigation into other frames of reference is left for future work. The *EFT* can be compared to a single flight with the same data post-processed with a set of only one, or a series of flights. We present the EFT post-processed comparison for flight data at launcher locations A and B. The comparison is made by wavenumber, so that the average velocity for a set of profiles is the *EFT* for a wavenumber of 0, and the velocity corresponding to a wave of period 5.0m is a wavenumber of 0.2/m. As the FFT is based on a sample frequency of 1.0m and a velocity profile with height 50.0m in this dataset, we can resolve a wavenumber up to 0.5/m

7.1 Launch location A

For a prevailing wind direction from the south (180T) we obtain for a single flight, comparison between the EFT of the IDDES CFD data as illustrated in Figure 14. A comparison of the EFT for a series of flights compared with the EFT for the CFD IDDES data for a wind direction of 180T at launcher location A is provided in Figure 15. For a westerly wind direction (270T) we obtain the comparison in Figure 14.

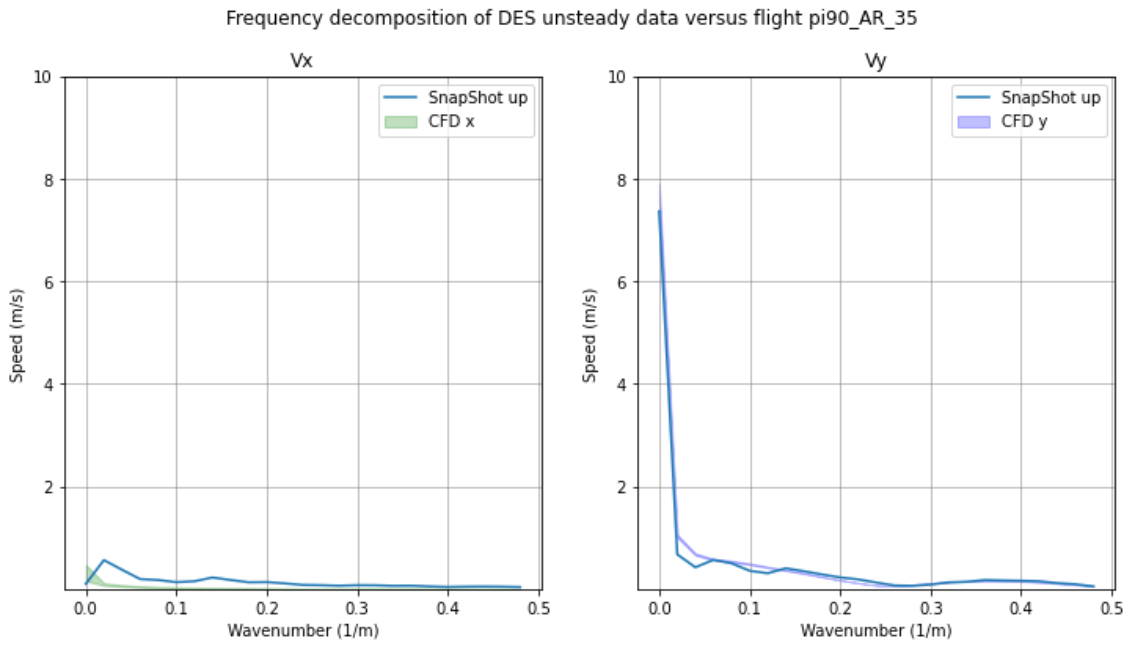

Figure 14: EFT comparison between the IDDES CFD velocity spectrum at launch location A for a southerly wind compared with flight "p90_AR_35." The mean wind speed is given by wavenumber=0, with increasing frequency resolution at higher wavenumbers. The IDDES CFD data is a mean value with a standard deviation above and below. Note that the standard deviation for the 1200 timesteps in the southerly wind direction is relatively small.

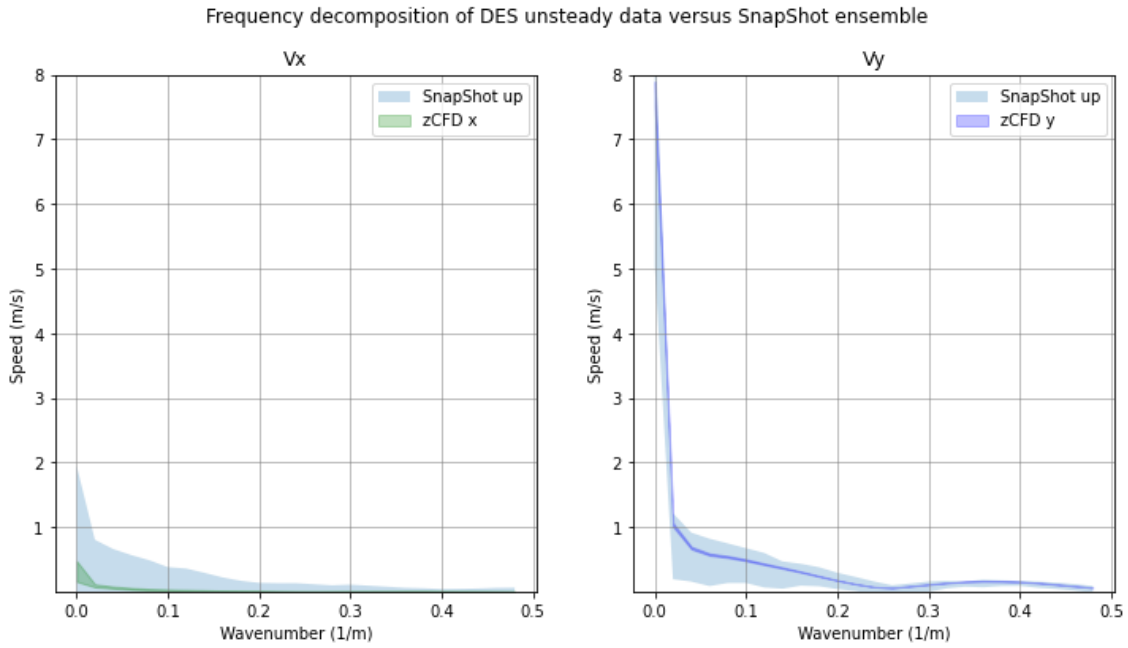

Figure 15: EFT comparison between the IDDES CFD velocity spectrum at launch location A for a southerly wind compared with EFT data for a series of 11 flights whose wind conditions match the IDDES CFD freestream conditions to within approximately 10 degrees and 1.5 m/s. As the number of flights increases the standard deviation becomes a statistically significant measure with which to compare the two sets of data.

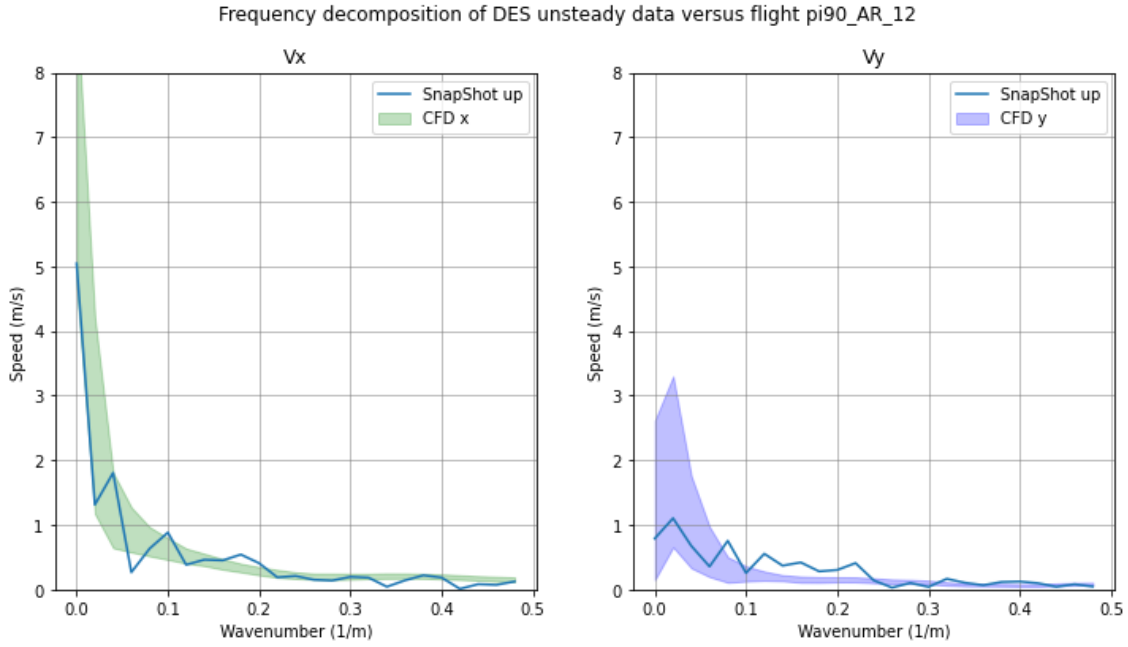

Figure 15: EFT comparison between the IDDES CFD velocity spectrum at launch location A for a westerly wind compared with flight “p90_AR_12.” The standard deviation for the 1200 timesteps in the westerly wind direction is relatively large as the flow on the leeward side of the BA Maintenance Hangar is more turbulent and complex. The flight data is reasonably well correlated with the frequency decomposition, though more flights are required to establish a statistically significant comparison.

7.2 Launch location B

Eight flights were recorded at launcher location B with a prevailing wind from the east (90T). An EFT comparison is illustrated for a single flight in Figure 17 and for the ensemble in Figure 18. The standard deviation for the 1200 timesteps in the easterly wind direction is smaller than for the westerly direction over the BA Maintenance Hangar but larger than for the southerly wind where there are no significant direct obstacles. This is as we might expect – the obstacles introduce large turbulent structures into the flow, which change the flow characteristics in the near-field. We would expect the flow downstream to return to a more homogeneous state in the absence of further large-scale perturbation. There is very good agreement between the IDDES CFD and the flight data.

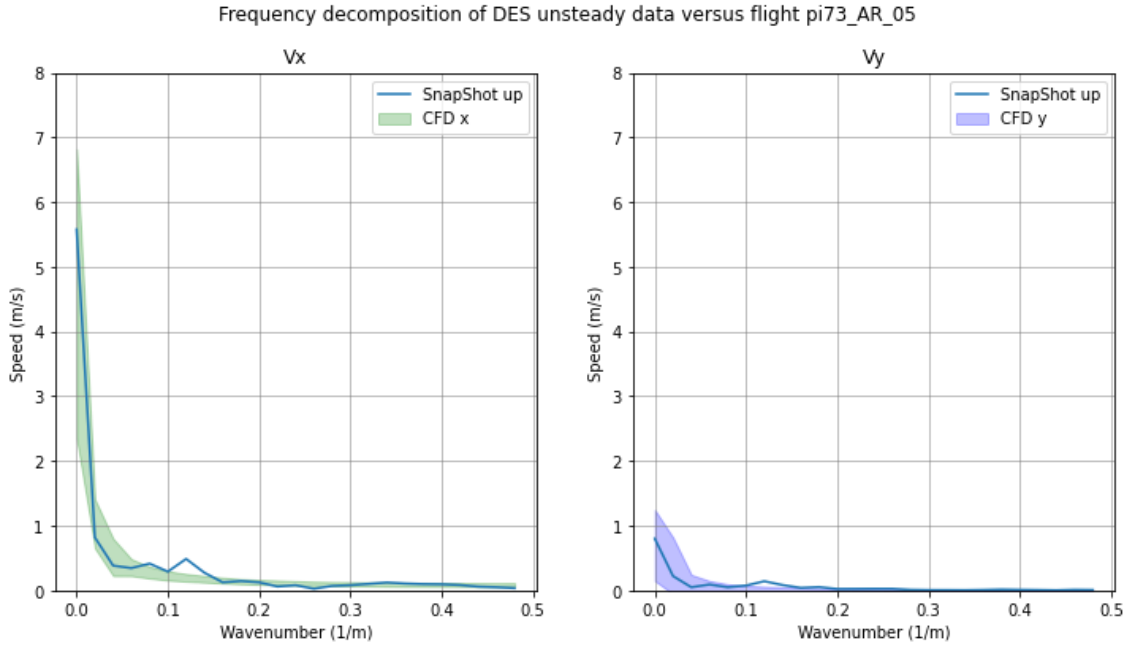

Figure 17: EFT comparison between the IDDES CFD velocity spectrum at launch location B for an easterly wind compared with flight "p73_AR_05."

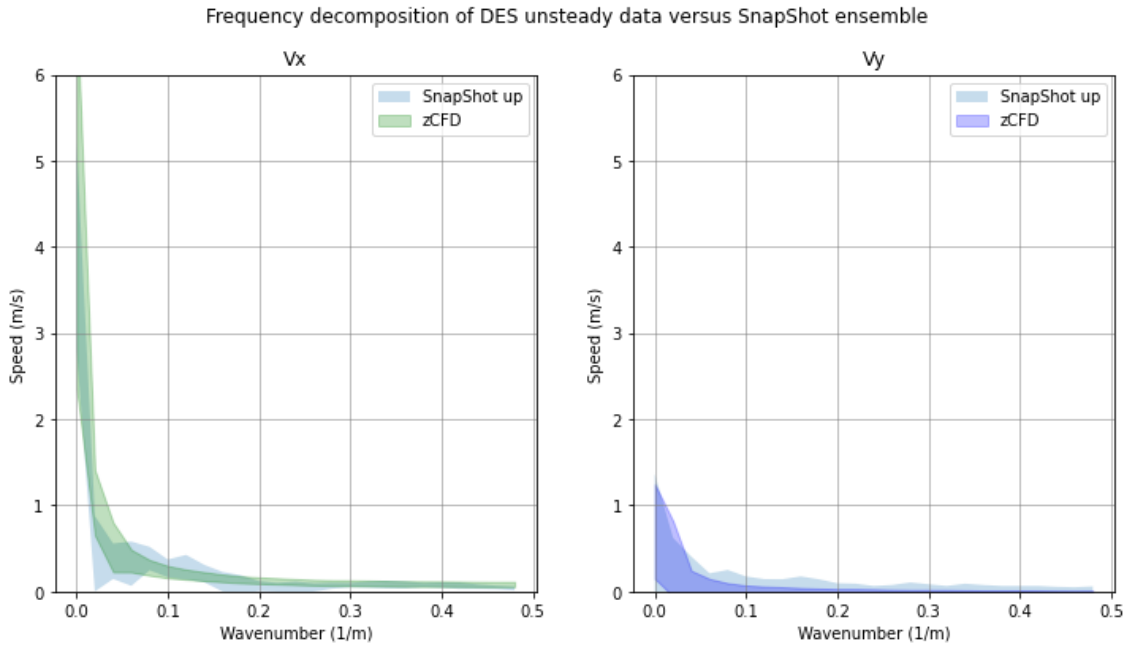

Figure 18: EFT comparison between the IDDES CFD velocity spectrum at launch location B for an easterly wind compared with the 8-flight ensemble. Both the mean values and the standard deviations for the datasets are in very good agreement.

8. Conclusions and recommendations

The present study broadly concludes that meaningful validation data for CFD-based airspace modelling can be provided by both static anemometers and the SnapShot wind measurement nano-glider. The two systems of direct measurement are complementary in nature, with the static anemometry providing long-term averaged data at a specific location, while SnapShot provides highly detailed flow field data on a specific trajectory at a certain point in time.

For averaged data comparisons aimed at establishing the bulk flow impact of nearby buildings, steady-state RANS CFD provides an informative and accurate model.

The use of the SnapShot data for validation of the CFD flow field depends upon the meso-scale conditions. For highly turbulent flow field on the leeward side of buildings, statistical analysis is required over an unsteady CFD dataset. The use of scale resolving IDDES CFD provides a suitable model, with excellent agreement on the mean and higher wavenumber flow features.

Further work is required to produced larger SnapShot experimental datasets and to establish the duration of the scale resolving unsteady CFD required for statistical convergence of the most aerodynamically meaningful data for drone operation.

9. Contact author email address

The corresponding author is David Standingford: david.standingford@zenotech.com.

10. Acknowledgement

We gratefully acknowledge support from UKRI Innovate UK under the “Future Flight challenge phase 2: strand 1, fast track development” project number 75307 “SafeZone: A dynamic safe zone system for autonomous urban flight.” We also gratefully acknowledge support for on-demand data production from the Aerospace Technology Institute / RIUK Innovate UK project number 113202 “Aerospace Cloud Services.”

11. Copyright statement

References

[1] Appa J, Turner M and Ashton N. *Performance of CPU and GPU HPC Architectures for off-design aircraft simulations*, AIAA 2021-0141, https://doi.org/10.2514/6.2021-0141, 2021.

[2] Wainwright T, Poole D, Allen C, Appa J and Darbyshire O. *High Fidelity Aero-Structural Simulation of Occluded Wind Turbine Blades*, AIAA 2021-0950, Session: Wind Turbine/Rotorcraft/Propeller Modeling Approaches. https://doi.org/10.2514/6.2021-0950, 2021.

[3] Standingford D. Rapid RANS wake simulation with customisable turbine models: CPU / GPU with Python interface. *WindEurope Conference, Poster Session PO175. Bilbao*, 2019.

[4] Saeed T, Walker S, Padhani S, Appa J and Allan M. *Affordable Modeling of Complex Extreme Events in the Built Environment Using GPU-accelerated CFD*, NVIDIA GTC, 2019.

[5] Lamb N, et al. Commercial and recreational drone use in the UK. House of Commons Science and Technology Committee. Twenty-Second Report of Session 2017–19. October 2019.

[6] Hetzler W and Ratti C, *Will delivery UAVs scale by 2030*? McKinsey and Company, August 2019.

[7] Baur S and Hader M, *Cargo Drones: The Urban Parcel Delivery Network of Tomorrow*, Roland Berger, 2020.

[8] Daniels C, *Autonomous nanodrone captures aerial intelligence in a snap*. DSEI London, 2021.

[9] UKRI, *Future Flight Vision and Roadmap*, UK Research and Innovation report UKRI-130821, August 2021.

[10] UKRI, Future Flight Challenge Socio-economic study, UK Research and Innovation report UKRI-120121, January 2021.

[11] Skylink. https://skyview-systems.co.uk/pages/skylink-pro

[12] Shur M L., Spalart P R, Strelets, M K, and Travin A K. A hybrid RANS-LES model with delayed DES and wall-modeled LES capabilities. *International Journal of Heat and Fluid Flow*, *29*, 1638–1649. doi: 10.1016/j.ijheatfluidflow.2008.07.00. 2008

[13] Natural Resource Wales, LIDAR Composite Dataset, https://lle.gov.wales/catalogue/item/LidarCompositeDataset

[14] Landberg L, *Meteorology for Wind Energy: An Introduction*, Wiley 2015.